CORE
Metadata, citation and similar papers at core.ac.uk
Provided by Tamkang University Institutional Repository

CHEMISTRY
A EUROPEAN JOURNAL
ChemPubSoc Europe

DOI: 10.1002/chem.201103423

Formation of Columnar Liquid Crystals on the Basis of Unconventional Triazine-Based Dendrimers by the C_3-Symmetric Approach

Long-Li Lai,*[a] Shun-Ju Hsu,[a] Hui-Chu Hsu,[a] Sheng-Wei Wang,[a] Kung-Lung Cheng,[b] Chun-Jung Chen,[c] Tsai-Hui Wang,[d] and Hsiu-Fu Hsu*[d]

Abstract: Two series of unconventional triazine-based dendrimers with C_2 symmetry and C_3 symmetry were prepared. The newly prepared C_3-symmetrical dendrimers were characterized by ^{1}H and ^{13}C NMR spectroscopy, mass spectrometry, and elemental analysis. Differential scanning calorimetry, polarizing microscopy, and powder XRD showed that the C_3-symmetrical dendrimers display columnar liquid-crystalline phases during thermal treatment, but the C_2-symmetrical dendrimers were not observed to behave correspondingly. The molecular conformations of C_3- and C_2-symmetrical dendrimers were obtained by computer simulation with the MM2 model of the CaChe program in the gas phase. The simulation results reasonably explain the different mesogenicities of C_3- and C_2-symmetric dendrimers. This new strategy should be applicable to other types of unconventional dendrimers with rigid frameworks for displaying columnar liquid-crystalline behavior.

Keywords: dendrimers · liquid crystals · molecular mechanics calculations · nitrogen heterocycles

Introduction

Dendrimers are starlike molecules in spheroidal or globular packing, often contain central cores, linkage units, and peripheral functional groups, and can be prepared by convergent, divergent, and combinatorial methods.[1] Particularly dendrimers combining monomolecular weight with interesting and predictable properties have emerged as an attractive research topic because they have potential to function as catalytic materials,[2] molecular micelles,[3] light-harvesting molecules,[4] drug-transport agents,[5] as well as porous and interfacial materials,[6] depending on their void spaces, sizes, and shapes. Dendrimers have also been observed to display columnar liquid-crystalline (LC) phases and have found uses in light-emitting diodes, photovoltaics, field transistors, and sensors,[7] because columnar liquid crystals (LCs) often have good charge-carrier mobility, no grain boundaries, and uniform alignment.[7d,8] Dendrimers that contain the triazine moiety have been extensively investigated. For example, Takagi et al. employed divergent and convergent methods to prepare disk-shaped dendrimers based on the triazine unit and aromatic linkage.[9] Simanek and co-workers also applied divergent, convergent, and combinatorial methods to prepare triazine-based dendrimers containing paclitaxcel or NH functionality in the peripheral parts for studying their transfection efficiency.[10a–c] Because more potential applications have been discovered for triazine-based dendrimers, various linkers for simplifying their synthesis or analysis were also recently reported.[10d,e] Interestingly, the triazine-based dendrimers were observed to show strong π–π interactions with tetrafluorobenzoquinone in solution, leading to significant redshift of UV absorbance (ca. 180 nm).[11] This indicates that the triazine moiety in the dendritic framework is suitable for face-to-face packing, which is an advantage for columnar LC formation.

However, unlike traditional disk-shaped compounds, which characteristically contain a rigid disklike central unit and a large number of surrounding flexible chains, dendrimers are more structurally versatile due to various repeating linkages between peripheral functional groups and central cores. It is therefore not so straightforward and predictable to control their molecular conformations for forming columnar LC phases as for traditional disk-shaped compounds.[12] Previously, dendritic LCs with columnar phases were often achieved by varying the peripheral alkyl chains or attaching peripheral mesogens to dendritic mainframes.[13] Induction of hydrogen-bonding interactions between dendrons, leading to formation of columnar LC phases, is also possible.[13,14].

[a] Prof. Dr. H.-L. Lai, S.-J. Hsu, H.-C. Hsu, S.-W. Wang
Department of Applied Chemistry, National Chi Nan University
No.1 University Rd., Puli, Nantou (Taiwan)
Fax: (+886) 49-2917956
E-mail: lilai@ncnu.edu.tw

[b] Dr. K.-L. Cheng
Material and Chemical Research Laboratories
Industrial Research Institute, Hsinchu (Taiwan)

[c] C.-J. Chen
Department of Chemistry, National Central University, Jhongli (Taiwan)

[d] T.-H. Wang, Prof. Dr. H.-F. Hsu
Department of Chemistry, Tamkang University, Tamsui (Taiwan)
E-mail: hhsu@mail.tku.edu.tw

Supporting information for this article is available on the WWW under http://dx.doi.org/10.1002/chem.201103423.

WILEY ONLINE LIBRARY
© 2012 Wiley-VCH Verlag GmbH & Co. KGaA, Weinheim

Recently, much study has focused on traditional disk-shaped compounds with C_3-symmetry because these materials efficiently self-assemble into columnar stacks and then show columnar LC phases due to intramolecular π–π and/or hydrogen-bonding interactions between molecules.[12,15] However, fewer examples of traditional molecules with C_2 symmetry showing columnar LC phases were reported, and they mostly focused on multiply hydrogen-bonded or macrocyclic compounds.[12,13] Introduction of chiral moieties into C_2-symmetrical molecules, leading to helical stacks by intramolecular π–π interaction and then showing columnar LC phases, was also reported.[16a] Deforming the planarity of trigonal molecules by strongly electron-withdrawing substituents or tilting bent molecules also resulted in columnar LC phases during the thermal processes.[15e,16b] Therefore, changing the planar shape of the rigid cores seems to be an efficient approach to molecules that exhibit columnar LC phases.

Previously, we prepared unconventional dendrimers $\mathbf{G_nN–NG_n}$ ($n=2$, 3) with C_2 symmetry, which characteristically have rigid central cores and rigid linkages but do not show columnar LC behavior during thermal treatment.[17] By expanding the C_2-to-C_3 concept of traditional disk-shaped compounds, we used tripiperazinyltriazine to replace piperazine as a central rigid core for preparing dendrimers with C_3 symmetry (Figure 1). Without introducing a chiral moiety into the dendritic framework, C_3-symmetrical dendrimers $\mathbf{(G_nN–N)_3T}$ ($n=2$, 3) were observed to display columnar LC phases during thermal treatment.

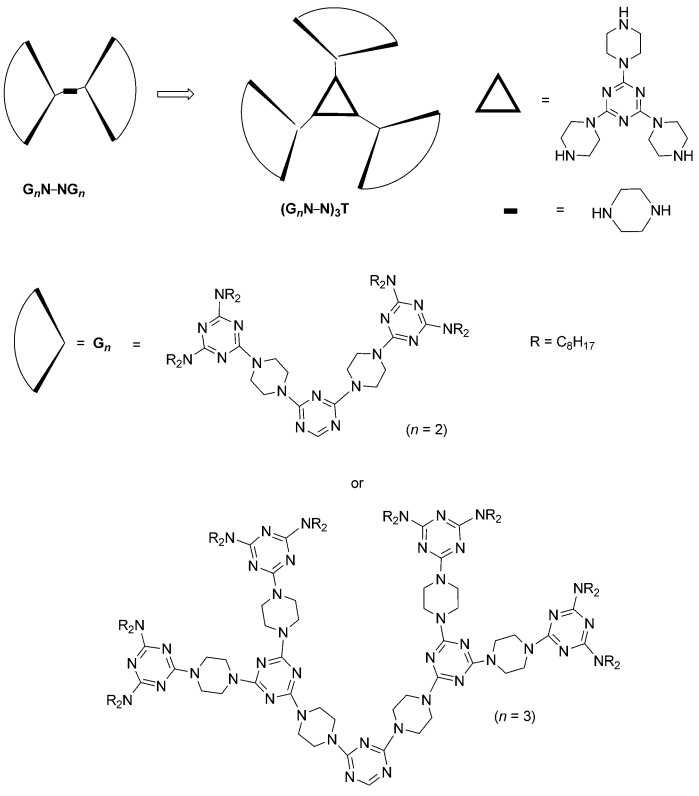

Figure 1. Structures of $\mathbf{G_nN–NG_n}$ and $\mathbf{(G_nN–N)_3T}$ ($n=2$, 3).

Results and Discussion

Dendrons **$G_2N–NH$**, **G_3Cl**, **$G_3N–NH$**, and **G_4Cl** were prepared according to literature procedures (Scheme 1).[17] The reaction of **$G_2N–NH$** with **G_3Cl** in THF in the presence of

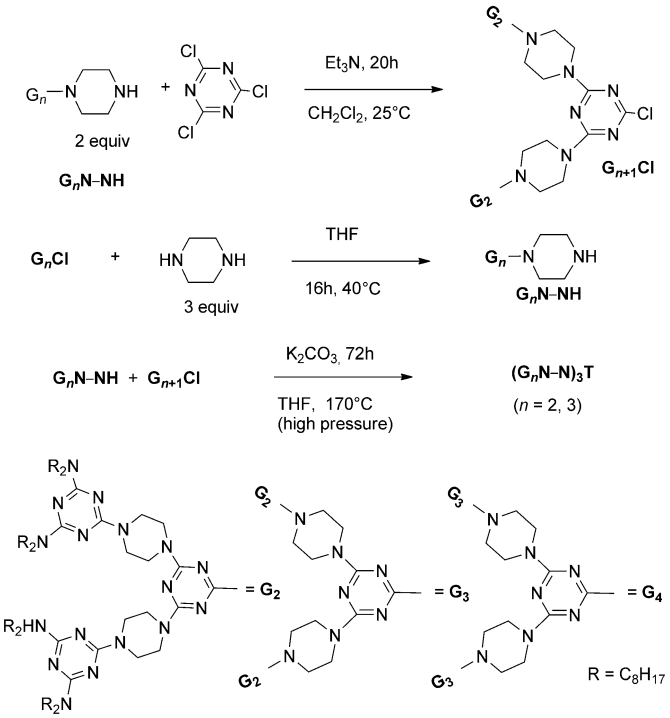

Scheme 1. Preparation of $\mathbf{(G_2N–N)_3T}$ and $\mathbf{(G_3N–N)_3T}$.

K_2CO_3 at 170 °C for 72 h in a sealed tube gave dendrimer $\mathbf{(G_2N–N)_3T}$ in about 50 % yield. In a similar manner, the reaction of **$G_3N–NH$** with **G_4Cl** gave dendrimer $\mathbf{(G_3N–N)_3T}$ in about 45 % yield. As indicated in the literature, the steric hindrance of functional groups in the peripheral part of dendrons impedes formation of dendrimers.[11] The steric hindrance of **$G_3N–NH$** and **G_4Cl** is greater than that of **$G_2N–NH$** and **G_3Cl**, and hence the yield of $\mathbf{(G_3N–N)_3T}$ is lower.

Dendrimers $\mathbf{(G_2N–N)_3T}$ and $\mathbf{(G_3N–N)_3T}$ were characterized by ^1H and ^{13}C NMR spectroscopy and mass spectrometry. The molecular structure of $\mathbf{(G_3N–N)_3T}$ is shown in Figure 2 (top). In its MALDI-TOF mass spectrum (Figure 2, bottom) a peak at 9248.02 for $[M]^+$ is clearly observed. Dendrimers $\mathbf{(G_2N–N)_3T}$ and $\mathbf{(G_3N–N)_3T}$ were further characterized by elemental analysis, and the errors for the calculated and experimental percentages of C, H, and N were within 0.3 %.

The LC properties of $\mathbf{G_nN–NG_n}$ and $\mathbf{(G_nN–N)_3T}$ ($n=2$, 3) are summarized in Table 1. For all of these compounds, no thermal decomposition was observed during the thermal processes. Dendrimer **$G_2N–NG_2$** only shows a melting point at about 131.5 °C on heating and a solidification point at about 116.5 °C on cooling. Similarly, dendrimer **$G_3N–NG_3$**

 © 2012 Wiley-VCH Verlag GmbH & Co. KGaA, Weinheim

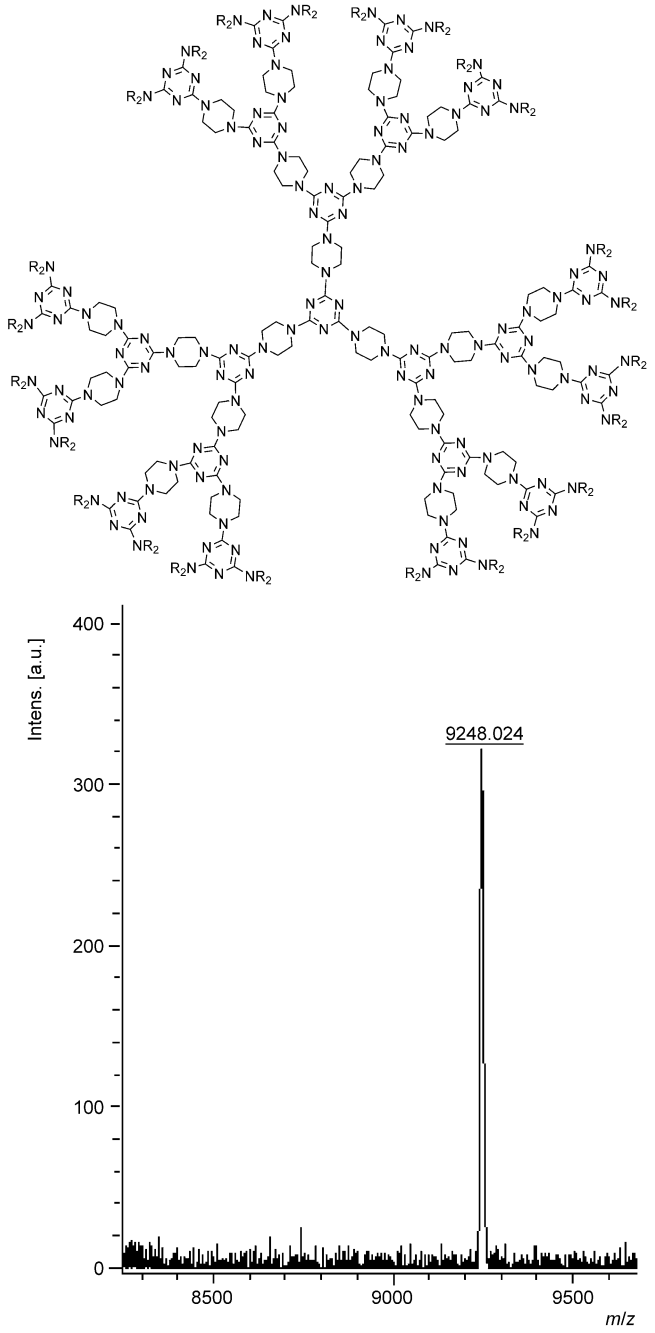

Figure 2. Molecular structure of $(\mathbf{G_3N–N)_3T}$ (top) and its mass spectrum (bottom).

shows a melting point at about 132.7 °C and a solidification point at about 97.6 °C on heating and cooling, respectively.

Dendrimer $\mathbf{(G_2N–N)_3T}$ displays a columnar LC phase during thermal processing, which is evidenced by its mosaic texture under a polarizing optical microscope (POM). The corresponding LC range is about 33 °C on heating and about 60 °C on cooling. The texture of $\mathbf{(G_3N–N)_2T}$ under the POM is rather irregular, which is not surprising, since the dendrimer contains a large amount of nonplanar structure in the peripheral part. The size of the larger domain is only about 24 μm (see Supporting Information). However, the sample

Table 1. Phase-transition temperatures and corresponding enthalpies [kJ mol^{-1}] in parentheses of dendrimers $\mathbf{G_nN–NG_n}$ and $\mathbf{(G_nN–N)_3T}$ ($n=2$, 3).[a]

$\mathbf{G_2N–NG_2}$ (MW = ca. 2813)	K	131.5 (107.7) / 112.6, 116.5 (-100.4) [b]				I
$\mathbf{G_3N–NG_3}$ (MW = ca. 6034)	K	128.2, 132.7 (171.4) [b] / 97.6 (-163.5)				I
$\mathbf{(G_2N–N)_3T}$ (MW = ca. 4423)	K	101.6 (5.2) [c] / 95.2, 102.8 (-39.3) [b]	$\mathbf{K_1}$	113.0 (20.5) [c]	$\mathbf{K_2}$	
	131.9 (42.2) [d] / 130.4 (-29.3) [e]	$\mathbf{K_3}$	140.5 (48.3) [d] / 135.6 (-38.2) [e]	$\mathbf{Col_r}$	172.5 (18.8) / 168.2 (-18.1)	I
$\mathbf{(G_3N–N)_3T}$ (MW = ca. 9248)	$\mathbf{K_1}$	154.8 (33.3) / 100.2 (-10.6)	$\mathbf{Col_r}$	137.0 [f]		I

[a] K, K_n ($n=1$–3), Col_r, and I denote the crystalline, rectangular columnar, and isotropic phases. The transition temperature and corresponding enthalpies were recorded for the second cycles between the isotropic and room temperatures. [b] Two transitions significantly overlapped; the enthalpies are integrated together. [c] Two transitions partially overlapped and the enthalpies are integrated individually. [d, e] show similar behavior and were processed similarly. The values when integrated together are shown in the Supporting Information. [f] The transition temperature was recorded by means of a polarizing optical microscope.

can be easily aligned between slides with rubbed PVA coatings to give a significantly expanded grain size of about 76 μm, desirable for bulk-property measurements. Accordingly, the size of the corresponding texture is more homogenous, indicative of regular alignment under such conditions (Figure 3). The identity of the columnar phase of $\mathbf{(G_2N–N)_3T}$ was further studied by powder XRD (Figure 4). Two sharp peaks at 33.58 and 28.55 Å, indexed as $d11$ and $d20$ respectively, are detected in the small-angle region and other weak signals at 20.77, 16.80, 14.22, and 13.44 Å are indexed as $d02$, $d22$, $d40$, and $d13$, respectively. The XRD pat-

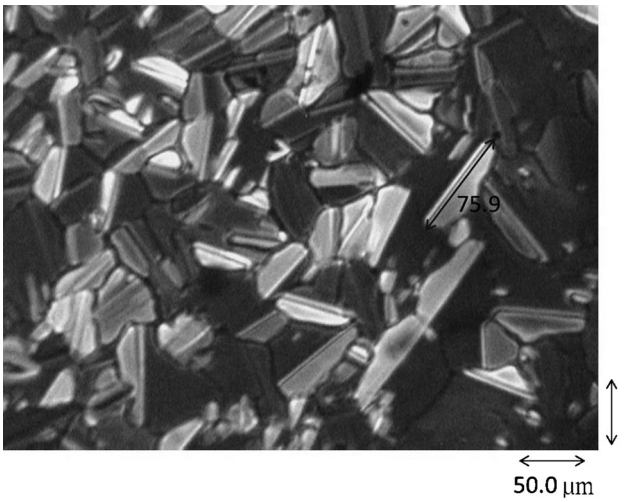

Figure 3. POM texture between slides with rubbed PVA coatings of $\mathbf{(G_2N–N)_3T}$ at 155 °C on cooling.

© 2012 Wiley-VCH Verlag GmbH & Co. KGaA, Weinheim

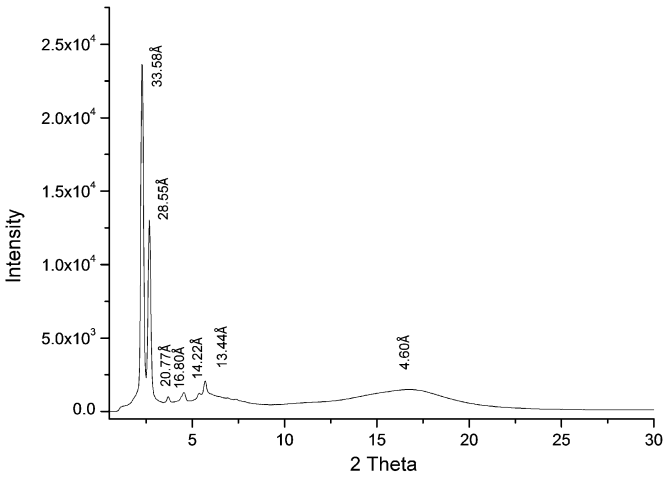

Figure 4. XRD pattern of $(G_2N–N)_3T$ at 155 °C on cooling.

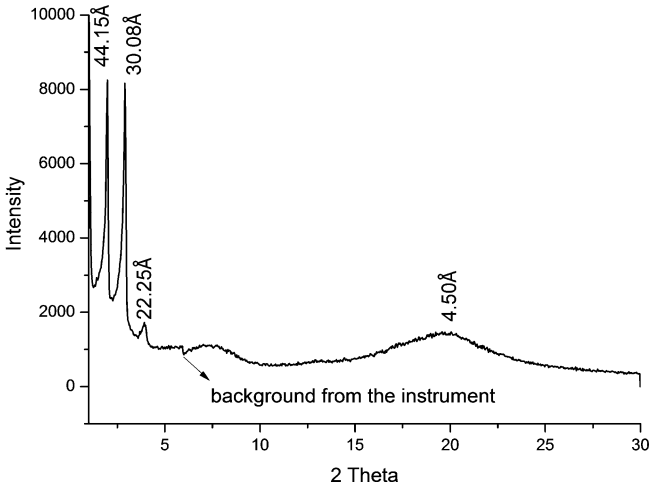

Figure 6. XRD pattern of $(G_3N–N)_3T$ at 110 °C on cooling.

tern is indicative of a rectangular columnar phase with *C2m* symmetry, and the calculated lattice constants are $a = 57.10$ and $b = 41.52$ Å. The wide-angle peak at 4.6 Å is attributed to the liquidlike correlation of the molten chains.

Under the POM, $(G_3N–N)_3T$ displays a columnar phase only in the cooling process, as evidenced by its mosaic texture (Figure 5). The corresponding mesogenic range is about 37 °C on cooling. Similarly, due to large amounts of nonplanar structure in the peripheral part, the optical texture of $(G_3N–N)_3T$ exhibits fine structures, and the size of the larger grains is determined to be about 49 μm (see Supporting Information). A more uniform texture with a significantly expanded average grain size of about 57 μm, desirable for bulk-property measurements, can be obtained by aligning the sample between rubbed slides.

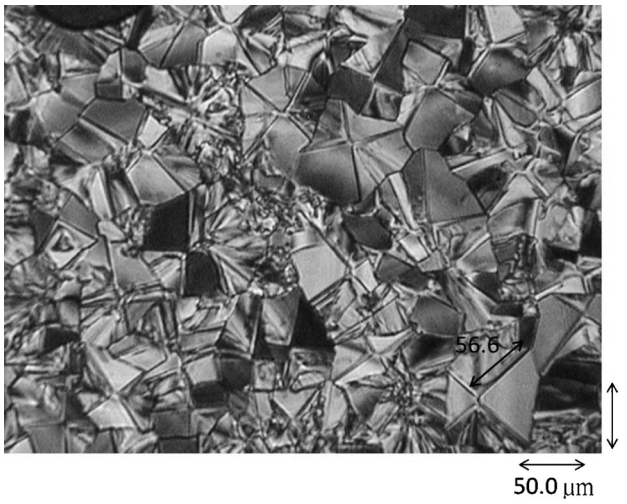

Figure 5. POM texture of $(G_3N–N)_3T$ between Kimwipes-rubbed slides at 110 °C on cooling.

The identity of the columnar phase of $(G_3N–N)_3T$ was further studied by powder XRD (Figure 6). Two sharp peaks at 44.15 and 30.88 Å are detected in the small-angle region and indexed as *d*11 and *d*20, respectively. Another weak XRD signal at 22.25 Å is indexed as *d*22. The XRD pattern is indicative of a rectangular columnar phase and the lattice constants are calculated to be $a = 60.16$ and $b = 64.99$ Å. Due to the lack of other reflections at wider angles, the symmetry of $(G_3N–N)_3T$ in the rectangular columnar phase was not determined. The wide-angle signal at 4.5 Å is attributed to the liquidlike correlation of the molten chains.

The packing of the dendrimers in the columnar phase can be further revealed by the 2D XRD patterns of $(G_2N–N)_3T$ and $(G_3N–N)_3T$, aligned by a 0.3 T magnetic-field (*B*). For both compounds under the applied field, the alignment of small-angle scatterings was not revealed (Figure 7), probably due to the high viscosity of the samples. On the other hand, wide-angle scatterings by alkyl chains are centered along the meridian, parallel to *B*. These results demonstrate that both dendrimers can be partially aligned on the alkyl parts but the packing of cores was not efficiently aligned to reveal the packing details due to the strong π–π interaction between the dendritic frameworks.

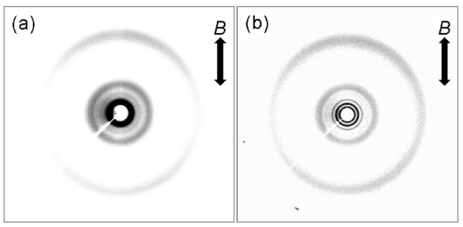

Figure 7. 2D XRD patterns of magnetic field aligned ($B = 0.3$ T) of a) $(G_2N–N)_3T$ at 155 °C and b) $(G_3N–N)_3T$ at 110 °C.

To visualize the molecular conformation of $G_nN–NG_n$ and $(G_nN–N)_3T$ ($n = 2, 3$), simulations were carried with CaChe by using MM2 model in the gas phase. The starting conformation of G_1-Cl was first established by combining one

 © 2012 Wiley-VCH Verlag GmbH & Co. KGaA, Weinheim

planar triazine with two dioctylamine moieties, whereby the linear alkyl chain is formulated in zigzag form, and then optimized. The conformation of **G_1-NH** was then obtained by combining optimized **G_1-Cl** with piperazine in chair form and then optimized. Similarly, the conformation of **G_2-Cl** was obtained by combining a planar triazine moiety with the two optimized **G_1-NH** units and then optimized. The optimized conformations of **G_2-NH**, **G_3-Cl**, **G_3-NH**, and **G_4-Cl** were obtained analogously. The conformation of **G_2N–NG_2** was obtained by combining optimized **G_2-Cl** with optimized **G_2-NH** and then optimized. The conformation of **G_3N–NG_3** was obtained by combining optimized **G_3-Cl** with optimized **G_3-NH** and then optimized. Accordingly, the conformations of **(G_2N–N)$_3$T** and **(G_3N–N)$_3$T** were obtained by combining optimized **G_3-Cl** with optimized **G_2-NH** and optimized **G_4-Cl** with optimized **G_3-NH**, respectively, and then optimized.

The optimized conformations of **G_2N–NG_2** and **G_3N–NG_3** in space-filling models are shown in Figure 8. For **G_2N–NG_2**, one **G_2** moiety partially lies above the other **G_2** moiety due

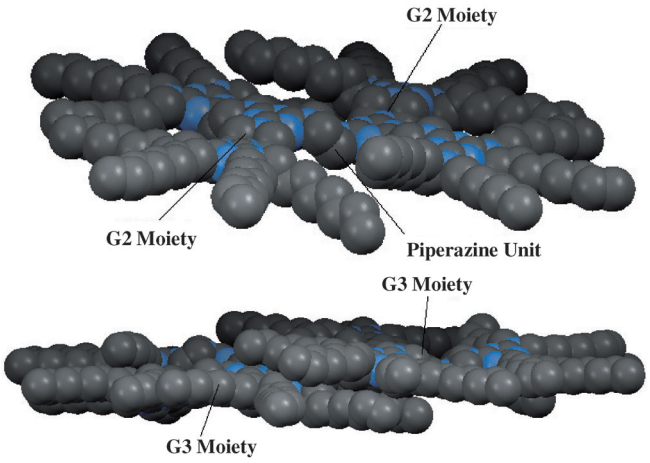

Figure 8. Conformations of **G_2N–NG_2** (top) and **G_3N–NG_3** (bottom); N blue, C gray, H omitted.

to the chair form of the central piperazine unit (Figure 8, top). The same situation is also found in the optimized conformation of **G_3N–NG_3** (Figure 8, bottom), but the central piperazine unit is completely hidden between two **G_3** moieties. Based on the computer simulation, dendrimers **G_2N–NG_2** and **G_3N–NG_3** are rather flat, and the molecular congestion of the peripheral alkyl chains and dendritic frameworks seems to be too weak to deform the molecular planarity. Therefore, the columnar LC phases were not generated during thermal processing, probably due to the strong π–π interaction between molecules.

The optimized conformations of **(G_2N–N)$_3$T** and **(G_3N–N)$_3$T** in space-filling models are shown in Figure 9. Interestingly, the molecular conformation of **(G_2N–N)$_3$T** is arranged as a three-leaf fan and leads to less π–π interaction between molecules. According to a detailed study of Percec and coworkers,[15g] dendrimers with C_3 symmetry and three-leaf fan conformation efficiently assemble into a columnar stacks

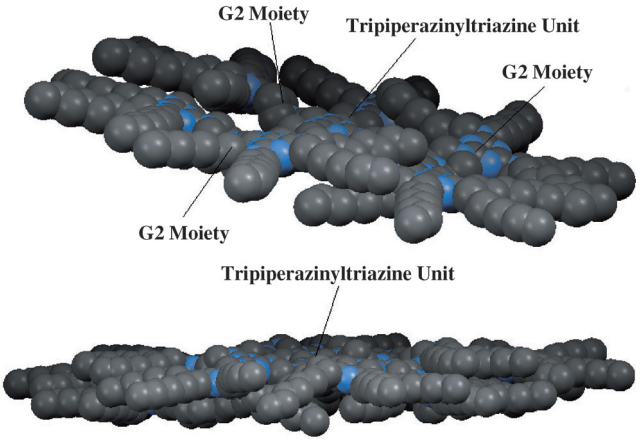

Figure 9. Conformations of (G_2N–N)$_3$T (top) and (G_3N–N)$_3$T (bottom); N blue, C gray, H omitted.

like traditional disk-shaped compounds with C_3 symmetry do.[15a–f] Thus, **(G_2N–N)$_3$T** shows a columnar LC phase during thermal treatment. The three-leaf fan conformation of **(G_3N–N)$_3$T** is not obvious, but according to the simulation, the congestion of **(G_3N–N)$_3$T** is significant, and leads to deformation of the molecular planarity and less molecular π–π interaction. The columnar LC phase of **(G_3N–N)$_3$T** is thus generated in the cooling process. According to the 2D XRD study, the viscosity of dendrimers in the LC state is still high, and indicates much higher π–π interaction in the corresponding crystalline state. Thus, the reduction of the dendritic π–π interaction seems to be important for formation of the LC phases during thermal processing, and our C_3-symmetry-adopting strategy is successful in inducing the columnar LC phases of dendritic molecules.

Conclusion

We prepared two new dendrimers **(G_2N–N)$_3$T** and **(G_3N–N)$_3$T** with C_3 symmetry, showing columnar LC phases during thermal processing. More homogenous alignment of **(G_2N–N)$_3$T** between slides with rubbed PVA coating and of **(G_3N–N)$_3$T** between rubbed slides was also achieved. On the basis of a simple molecular simulation in the gas phase and the work of Percec et al.,[15g] we reasonably explain why dendrimers **G_2N–NG_2** and **G_3N–NG_3** with C_2 symmetry do not display LC phases and why dendrimers **(G_2N–N)$_3$T** and **(G_3N–N)$_3$T** with C_3 symmetry do show columnar LC phases during thermal processing. Although dendrimers with C_2 or C_3 symmetry are well-known,[5] to the best of our knowledge, this is the first systematic comparison of differences in mesogenicity between the corresponding analogous dendrimers. It is noteworthy that the molecular weight of **(G_2N–N)$_3$T** is between those of **G_2N–NG_2** and **G_3N–NG_3**, that is, the molecular conformation but not the size of the dendrimers is important in inducing their mesogenic phases. Adoption of the C_2-to-C_3 concept for preparing columnar LCs in our approach is successful and should be applicable

 © 2012 Wiley-VCH Verlag GmbH & Co. KGaA, Weinheim

to other types of unconventional dendrimers with rigid frameworks.

Experimental Section

Preparation of $(G_2N–N)_3T$: **C_8G_3Cl** (3.00 g, 1 mmol), **C_8G_2NH** (1.45 g, 1 mmol), and K_2CO_3 (0.5 g, 5 mmol) were added to THF (15 mL) in a sealed tube. The resulting mixture was heated at 170 °C for 72 h. Water (50 mL) was added and the resulting mixture was extracted with CH_2Cl_2 (2×30 mL). The combined organic extracts were further washed with aqueous KOH solution (50 mL, pH 10) and then water (50 mL) and dried over magnesium sulfate. The solvent was removed under reduced pressure and the residue was then purified by chromatography on silica to give **$(G_2N–N)_3T$** in 50.4% yield (2.21 g). ^{1}H NMR (300 MHz, $CDCl_3$, 25 °C, TMS): δ = 0.89 (t, J (H,H) = 6.6, 72H, 24×CH_3), 1.29 (brs, 240H, 120×CH_2), 1.51–1.58 (m, 48H, 24×CH_2), 3.46 (brs, 28H, 24×CH_2), 3.80 + 3.82 ppm (2s, 72H, 36×CH_2); ^{13}C NMR (75 MHz, $CDCl_3$, 25 °C, TMS): δ = 14.08, 22.84, 27.32, 27.54, 28.32, 28.46, 29.47, 29.65, 29.84, 32.07, 43.31, 47.08, 47.36, 165.26, 165.58, 165.63 ppm; MS calcd for $C_{258}H_{480}N_{60}$ $[M]^+$: 4423.0; found: 4422.9; elemental analysis (%) calcd for $C_{258}H_{480}N_{60}$: C 70.06, H 10.94, N 19.0; found: C 70.09, H 10.98, N 18.87.

Preparation of $(G_3N–N)_3T$: **C_8G_4Cl** (6.23 g, 1 mmol), **C_8G_3NH** (3.06 g, 1 mmol), and K_2CO_3 (0.5 g, 5 mmol) were added to THF (15 mL) in a sealed tube. The resulting mixture was heated at 170 °C for 72 h. Water (50 mL) was added and the resulting mixture was extracted with CH_2Cl_2 (2×30 mL). After normal workup as described above, **$(G_3N–N)_3T$** was obtained in 45.2% yield (4.16 g). ^{1}H NMR (300 MHz, $CDCl_3$, 25 °C, TMS): δ = 0.88 (t, J (H,H) = 6.3, 96H, 48×CH_3), 1.29 (brs, 480H, 240×CH_2), 1.59 (brs, 96H, 48×CH_2), 3.46 (brs, 96H, 48×CH_2), 3.80 + 3.84 ppm (2s, 168H, 84×CH_2); ^{13}C NMR (75 MHz, $CDCl_3$, 25 °C, TMS): δ = 14.07, 22.68, 27.16, 27.37, 28.17, 28.31, 29.31, 29.49, 29.67, 31.91, 43.16, 46.95, 47.21, 165.07, 165.40, 165.46, 165.61 ppm; MS calcd for $C_{534}H_{984}N_{132}$ $[M]^+$: 9248.1; found: 9248.0; elemental analysis (%) calcd for $C_{534}H_{984}N_{132}$: N 19.98, C 69.30, H 10.72; found N 19.92, C 69.35, H 10.79.

Acknowledgements

We thank the National Chi Nan University and the National Science Council (NSC 98-2119-M-260-003 and NSC 100-2113-M-260-006-MY2) for financial support.

[1] G. R. Newkome, C. N. Moorefield, F. Vögtle, *Dendrimers and Dendrons*, Wiley-VCH, Weinheim, **2000**.

[2] a) J. P. K. Reynhardt, Y. Yang, A. Sayari, H. Apler, *Chem. Mater.* **2004**, *16*, 4095–4102; b) S. Javor, E. Delort, T. Darbre, J.-L. Reymond, *J. Am. Chem. Soc.* **2007**, *129*, 13238–13246; c) X. Peng, Q. Pan, G. L. Rempel, *Chem. Soc. Rev.* **2008**, *37*, 1619–1628; d) J. Yu, T. V. RajanBabu, J. R. Parquette, *J. Am. Chem. Soc.* **2008**, *130*, 7845–7847.

[3] a) J. F. G. A. Jansen, E. M. M. de Brabander-van den Berg, E. W. Meijer, *Science* **1994**, *266*, 1226–1229; b) N. Canilho, E. Kasëmi, A. D. Schlüter, J. Ruokolainen, R. Mezzenga, *Macromolecules* **2007**, *40*, 7609–7616.

[4] a) D. L. Jiang, T. Aida, *Nature* **1997**, *388*, 454–456; b) M. Kimura, T. Shiba, T. Muto, K. Hanabusa, H. Shirai, *Macormolecules* **1999**, *32*, 8237–8239.

[5] a) M. Gingras, J.-M. Raimundo, Y. M. Chabre, *Angew. Chem.* **2007**, *119*, 1028–1035; *Angew. Chem. Int. Ed.* **2007**, *46*, 1010–1017; b) Y. Kim, A. M. Klutz, K. A. Jacobson, *Bioconjugate Chem.* **2008**, *19*, 1660–1672.

[6] a) K. Landskron, G. A. Ozin, *Science* **2004**, *306*, 1529–1532; b) M. S. Kaucher, M. Peterca, A. E. Dulcey, A. J. Kim, S. A. Vinogradov, D. A. Hammer, P. A. Heiney, V. Percec, *J. Am. Chem. Soc.* **2007**, *129*, 11698–11699.

[7] a) L. Schmidt-Mende, A. Fechtenkotter, K. Müllen, E. Moons, R. H. Friend, J. D. MacKenzie, *Science* **2001**, *293*, 1119–1122; b) R. Freudenmann, B. Behnisch, M. Hanack, *J. Mater. Chem.* **2001**, *11*, 1618–1624; c) N. Boden, R. J. Bushby, J. Clements, B. Movaghar, *J. Mater. Chem.* **1999**, *9*, 2081–2086; d) A. M. Van de Craats, N. Stutzmann, O. Bunk, M. M. Nielsen, M. Watson, K. Müllen, H. D. Chanzy, H Sirringhaus, R. H. Friend, *Adv. Mater.* **2003**, *15*, 495–499.

[8] a) W. Pisula, A. Menon, M. Stepputat, I. Lieberwirth, U. Kolb, A. Tracz, H. Sirringhaus, T. Pakula, K. Müllen, *Adv. Mater.* **2005**, *17*, 684–689; b) W. Pisula, Z. Tomovic, B. El Hamaoui, M. D. Watson, T. Pakula, K. Müllen, *Adv. Funct. Mater.* **2005**, *15*, 893–904; c) E. J. Foster, R. B. Jones, C. Lavigueur, V. E. Williams, *J. Am. Chem. Soc.* **2006**, *128*, 8569–8574.

[9] K. Takagi, T. Hattori, H. Kunisada, Y. Yuki, *J. Polym. Sc. Part A* **2000**, *38*, 4385–4395.

[10] a) M. B. Steffensen, E. Hollink, F. Kuschel, M. Bauer, E. E. Simanek, *J. Polym. Sc. Part A* **2006**, *44*, 3411–3433; b) J. Lim, E. E. Simanek, *Org. Lett.* **2008**, *10*, 201–204; c) M. A. Mintzer, O. M. Merkel, T. Kissel, E. E. Simanek, *New J. Chem.* **2009**, *33*, 1918–1925; d) M. A. Mintzer, L. M. Perez, E. E. Simanek, *Tetrahedron Lett.* **2010**, *51*, 1631–1634; e) J. Lim, M. A. Mintzer, L. M. Perez, E. E. Simanek, *Org. Lett.* **2010**, *12*, 1148–1151.

[11] L. L. Lai, H.-C. Hsu, S.-J. Hsu, K. L. Cheng, *Synthesis* **2010**, 3576–3582.

[12] a) C. Tschierske, *Annu. Rep. Prog. Chem. Sect. C* **2001**, *97*, 191–267; b) X. Feng, W. Pisula, M. Takase, X. Dou, V. Enkelmann, M. Wagner, N. Ding, K. Müllen, *Chem. Mater.* **2008**, *20*, 2872–2874; c) X. Feng, W. Pisula, T. Kudernac, D. Wu, L. Zhi, S. De Feyter, K. Müllen, *J. Am. Chem. Soc.* **2009**, *131*, 4439–4448.

[13] a) I. M. Saez, J. W. Goodby, *J. Mater. Chem.* **2005**, *15*, 26–40; b) B. Bertrand, D. Guillon, *Adv. Polym. Sci.* **2006**, *201*, 45–155; c) T. Kato, N. Mizoshita, K. Kishimoto, *Angew. Chem.* **2006**, *118*, 44–74; *Angew. Chem. Int. Ed.* **2006**, *45*, 38–68; d) M. Marcos, R. Martín-Rapúm, A. Omenta, J. L. Serrano, *Chem. Soc. Rev.* **2007**, *36*, 1889–1901; e) G. C. Shearman, G. Yahioglu, J. Kirstein, L. R. Milgrom, J. M. Seddon, *J. Mater. Chem.* **2009**, *19*, 598–604.

[14] a) C. M. Paleos, D. Tsiourvas, *Liq. Cryst.* **2001**, *28*, 1127–1161; b) G.-C. Kuang, Y. Ji, X.-R. Jia, Y. Li, E.-Q. Chen, Y. Wei, *Chem. Mater.* **2008**, *20*, 4173–4175.

[15] a) M. M. J. Smulders, A. P. H. J. Schenning, E. W. Meijer, *J. Am. Chem. Soc.* **2008**, *130*, 606–611; b) J. van Gestel, A. R. A. Palmans, B. Titulaer, J. A. J. M. Vekemans, E. W. Meijer, *J. Am. Chem. Soc.* **2005**, *127*, 5490–5494; c) R. Martín-Rapún, D. Byelov, A. R. A. Palmans, W. H. de Jeu, E. W. Meijer, *Langmuir* **2009**, *25*, 8794–8801; d) X. Feng, W. Pisula, L. Zhi, M Takase, K. Müllen, *Angew. Chem.* **2008**, *120*, 1727–1730; *Angew. Chem. Int. Ed.* **2008**, *47*, 1703–1706; e) Z. Li, L. Zhi, N. T. Lucas, Z. Wang, *Tetrahedron* **2009**, *65*, 3417–3424; f) M. H. C. J. van Houtem, R. Martin-Rapun, J. A. J. M. Vekemans, E. W. Meijer, *Chem. Eur. J.* **2010**, *16*, 2258–2271; g) M. Peterca, M. R. Imam, C.-H. Ahn, V. S. K. Balagurusamy, D. A. Wilson, B. M. Rosen, V. Percec, *J. Am. Chem. Soc.* **2011**, *133*, 2311–2328.

[16] a) C.-W. Yang, T.-H. Hsia, C.-C. Chen, C.-K. Lai, R.-S. Liu, *Org. Lett.* **2008**, *10*, 4069–4072; b) N. Vaupotič, D. Pociecha, M. Cepic, K. Gomola, J. Mieczkowski, E. Gorecka, *Soft Matter* **2009**, *5*, 2281–2285.

[17] a) L. L. Lai, L. Y. Wang, C. H. Lee, Y. C. Lin, K. L. Cheng, *Org. Lett.* **2006**, *8*, 1541–1544; b) L. L. Lai, C. H. Lee, L. Y. Wang, K. L. Cheng, H.-F. Hsu, *J. Org. Chem.* **2008**, *73*, 485–490.

Received: October 31, 2011
Published online: April 4, 2012

 © 2012 Wiley-VCH Verlag GmbH & Co. KGaA, Weinheim